sustainability

MDPI

Article

Macro- and Micro-Characteristics and Mechanical Properties of Xigeda Formation Claystone in Luding County, Western Sichuan, China

Ruian Wu [1,2,*], Xiang Li [1,3,*], Changbao Guo [1,2], Jiawei Ni [1,4], Yang Wang [1,2], Deguang Song [1] and Chang Qi [1,4]

[1] Institute of Geomechanics, Chinese Academy of Geological Sciences, Beijing 100081, China
[2] Key Laboratory of Active Tectonics and Geological Safety, Ministry of Natural Resources, Beijing 100081, China
[3] School of Engineering, China University of Geosciences, Wuhan 430074, China
[4] School of Engineering and Technology, China University of Geosciences, Beijing 100083, China
* Correspondence: wuruian1991@126.com (R.W.); lix1228@cug.edu.cn (X.L.)

Abstract: Claystone is actually a type of hard soil or soft rock. To reveal the engineering geological characteristics of the Xigeda formation claystone in Luding County (Western Sichuan, China), some experiments, including X-ray diffraction (XRD), scanning electron microscopy (SEM), and geotechnical tests, are performed. The testing results indicate that the Xigeda formation claystone primarily consists of silt, clay, and other fine-grained materials. It is characterized by interbedded yellow and gray thin layers with a horizontal lamination structure. The yellow and gray claystones are made of the same materials but differ in their proportions. Additionally, yellow claystone is characterized by a higher density, resulting in enhanced cementation among clay particles. The permeability coefficient of Xigeda formation claystones ranges from 3.62×10^{-4}~7.34×10^{-4} cm/s. The cohesion of yellow and gray claystones decreases with increasing moisture content, and the decline is greater at higher moisture contents. However, the relationship between internal friction angle and moisture content is different. The mechanical properties of the Xigeda formation exhibit significant differences in sensitivity to changes in moisture content across various regions. Notably, the claystone within the study region experiences a particularly pronounced weakening of its mechanical properties when exposed to water.

Keywords: hard soil and soft rock; geotechnical test; microstructure; permeability; mechanical property

Citation: Wu, R.; Li, X.; Guo, C.; Ni, J.; Wang, Y.; Song, D.; Qi, C. Macro- and Micro-Characteristics and Mechanical Properties of Xigeda Formation Claystone in Luding County, Western Sichuan, China. *Sustainability* **2023**, *15*, 13274. https://doi.org/10.3390/su151713274

Academic Editor: Marco Lezzerini

Received: 20 July 2023
Revised: 24 August 2023
Accepted: 28 August 2023
Published: 4 September 2023

1. Introduction

The study of claystone has been extensively conducted by numerous scholars since the 1970s. Typically, these materials, known as hard soil and soft rock, are classified based on their uniaxial compressive strength [1–3]. A large number of field investigations, geotechnical tests, and engineering construction practices have consistently demonstrated that hard soil and soft rock exhibit characteristics such as expansion and contraction, multiple fractures, and overconsolidation. Furthermore, these materials are prone to displaying engineering properties of low strength, substantial deformation, and susceptibility to softening and becoming muddy upon contact with water [4–7]. The presence of hard soil and soft rock can create favorable conditions for the occurrence of geological hazards as well as pose challenges in terms of engineering geology [8–10].

The Xigeda formation (NQx) is a distinctive type of hard soil and soft rock material with a unique geological structure. In China, the majority of scholars classify the Xigeda formation as semi-diagenetic [11]. It represents a late Cenozoic stratigraphic unit found in southwestern China, primarily distributed within major river systems such as the Jinsha River, Dadu River, and Anning River and their associated tributary valleys, fault valleys, or erosional depressions (Figure 1). The Xigeda formation primarily consists of fine-grained

materials, such as clay, silt, and fine sand, exhibiting a horizontal bedding structure [11–14]. This set of formations exhibits unfavorable engineering geological characteristics while also serving as a potential source for geological hazards [15,16]. For instance, during the tunnel construction of the Chengdu-Kunming Railway through the Xigeda formation, some problems, such as vault settlement, base subsidence, local wetting instability, and collapse, were encountered in the surrounding rock [15]. The landslide that occurred in Zhonghai Village, Hanyuan County, Sichuan Province, within the Xigeda formation has resulted in an interruption to the S360 provincial highway, leading to seven fatalities, two missing individuals, and eight destroyed houses [16].

Figure 1. Distribution of Xigeda formation, southwestern China.

Currently, a multitude of scholars have conducted extensive research on the Xigeda formation in southwestern China and have made significant progress [11,17–19]. The previous studies have demonstrated significant variations in the mineral composition and material of the Xigeda formation across different regions, wherein physical and mechanical properties, as well as hydrophysical characteristics, exhibit close associations with these regional disparities. The Xigeda formation exhibits good self-stability under natural conditions but is highly susceptible to water influence. The mechanical strength experiences a sudden decrease once the moisture content exceeds its sensitive threshold. The development of geological hazards in the Xigeda formation is influenced by factors such as soil moisture content and the characteristics of internal joints and fractures. The primary structural planes responsible for landslides are located at the contact interface between the Xigeda formation and the overlying loose accumulation layer, as well as within underlying layers and soft sedimentary structure planes within these layers. The aforementioned research indicates significant variations in the material composition and rock-soil properties of the Xigeda formation across different regions. In its natural state, this formation exhibits favorable engineering characteristics and self-stability. However, excessive moisture content beyond a certain threshold can lead to substantial attenuation of its strength, thereby increasing the likelihood of geological hazards and engineering geology problems. The engineering and geological problems caused by the Xigeda formation are becoming increasingly prominent due to escalating human activities [15]. The investigation of the engineering and geological characteristics of this unique hard soil and soft rock formation is therefore highly significant.

In this study, we focus on the claystone of the Xigeda formation located in Haiziping Village, Luding County, Sichuan Province, China. Based on XRD and SEM analyses, the material composition and microstructure characteristics of the claystone were examined. In-situ permeability tests and laboratory mechanical tests were conducted to investigate the hydraulic and mechanical properties of the Xigeda formation, which were then compared with those of other regions in southwestern China. These findings have significant implications for further research into the hard soil and soft rock as well as supporting local geological hazard prevention and mitigation efforts.

2. Background of the Study Site

On the right bank of the Dadu River in Haiziping Village, Luding County, a series of seven fluvial terraces have been observed. The Xigeda formation is situated above the T3 terrace and has an exposed thickness of approximately 440 m, rendering it the most extensive sedimentary section of the Xigeda formation ever documented in China (Figure 2). The elevations of T4–T7 terraces, based on the Xigeda formation, are 770 m, 820 m, 880 m, and 930 m, respectively. In the Dadu River valley, T1–T3 terraces were identified with elevations of 10 m, 50 m, and 100 m, respectively (Figure 3). Notably, there is a relative height difference of up to 670 m between T3 and T4.

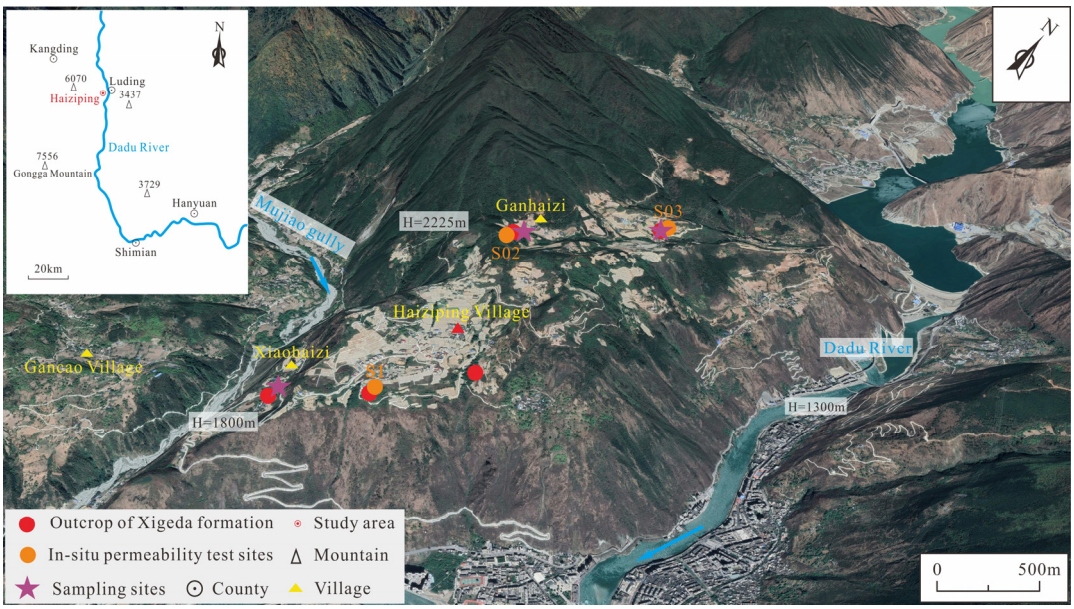

Figure 2. Distribution of Xigeda formation in Haiziping Village, Luding County, western Sichuan.

The Xigeda formation in Haiziping Village, Luding County, consists of interbedded yellow and gray claystones (Figure 4). At the base of this formation, there are breccia and gravel layers that exhibit angular unconformity with the underlying bedrock. Due to tectonic activity, the Xigeda formation as a whole is inclined towards the west at an angle of approximately 10~20°, locally reaching up to 30° [12]. Under the influence of vegetation, weathering and erosion, human engineering activities, and other factors, the continuity of outcrop conditions for the Xigeda formation in Haiziping Village is poor and only occurs sporadically in Xiaohaizi, Ganhaizi, and other locations. After conducting a field investigation, it has been observed that a multitude of shallow landslides and debris are present within this formation. Under the circumstances of excessive rainfall, some landslides may experience post-failure mobilization along the gully and rapidly transform into debris flows, causing certain damage to the outlet of the gully [20].

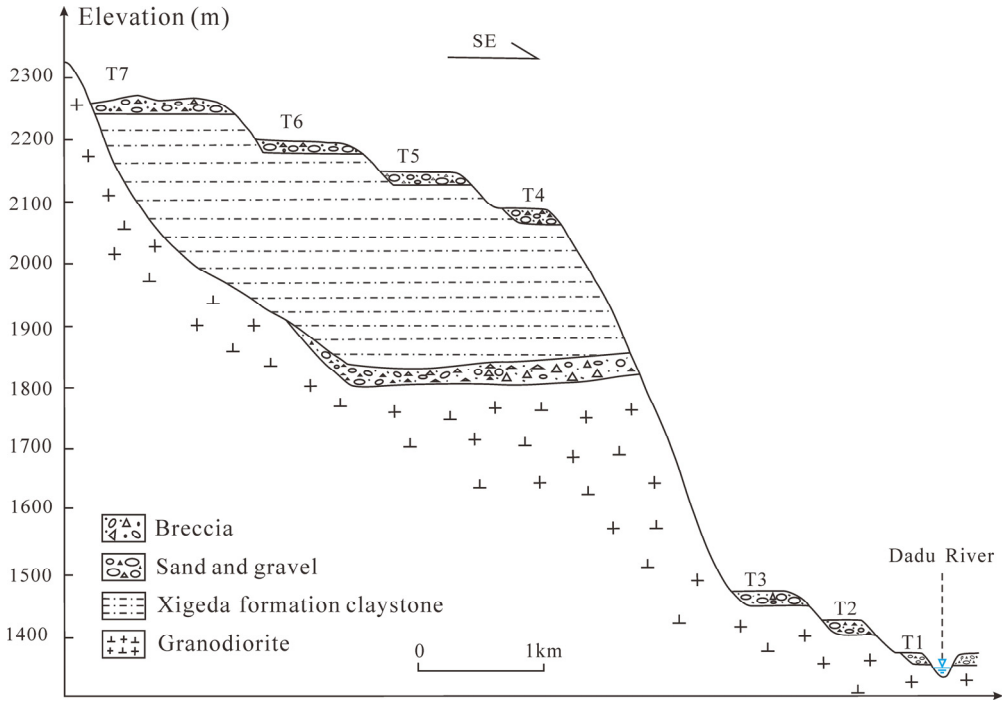

Figure 3. Geological profile of the Dadu River terrace in Haiziping Village, Luding County (modified from Jiang et al. [12]).

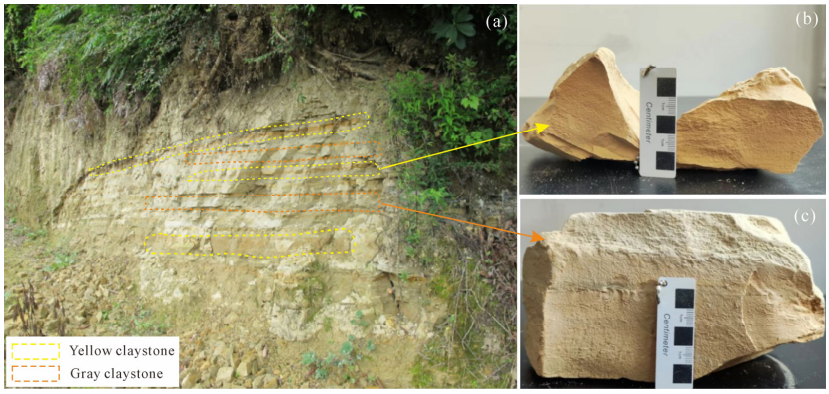

Figure 4. Development characteristics of claystone in Haiziping Village, Luding County: (**a**) exposure profile of the Xigeda Formation claystone in Haiziping Village; (**b**) Yellow claystone sample; (**c**) Gray claystone sample.

In terms of the formation mechanism of the Xigeda formation, several hypotheses have been proposed, including glacial-lake deposition, fault lake deposition, barrier lake deposition, panlacustrine deposition, and intermountain basin [12,21–23]. The genetic mechanism of the Xigeda formation in Haiziping Village is primarily classified into two types: faulted basin and barrier lake [12,21]. The field investigation reveals a significant development of large-scale and giant ancient landslides in the Luding County-Detuo Town section of the Dadu River basin, with historical evidence indicating that most of these landslides have obstructed the Dadu River [24,25]. Therefore, it is believed that the Xigeda formation in Haiziping Village, Luding County, is more likely to be sediment that accumulated after the landslide blocked the river. In the exploration of its formative chronology, diverse scholars have employed a plethora of dating techniques, including paleomagnetic, optically stimulated luminescence (OSL), electron spin resonance (ESR), cosmogenic nuclides, and others, to ascertain a wide range of ages (Table 1).

Table 1. The dating methods and statistical results of Xigeda formation in Haiziping Village, Luding County.

Dating Method	Test Age (Ma)	Data Source
Paleomagnetism	4.20~2.60	Reference [12]
OSL	1.78~1.13	Reference [21]
ESR	0.70~0.40	Reference [19]
Cosmogenic nuclides	1.04~0.53	Reference [20]

3. Materials and Methods

3.1. Sample Material and Preparation

The experimental samples were collected from the Xigeda formation located in fluvial terraces T4–T6 of Haiziping Village, Luding County (Figure 4). These samples consist of yellow and gray claystones. According to the Standard of Geotechnical Test Method [26], the yellow and gray claystone samples are processed by drying, pulverizing, and sieving, followed by a series of physical property tests. Parameters such as natural moisture content, specific gravity of soil particles, natural density, dry density, porosity ratio, liquid limit moisture content, plastic limit moisture content, and saturated moisture content were obtained.

3.2. X-ray Diffraction Tests

X-ray diffraction analysis is a physical method that utilizes the diffraction effect of X-rays interacting with mineral crystals to analyze their structure and phase [27]. It serves as an essential technical means for identifying minerals. Additionally, the Reference Intensity Ratio (RIR method, also known as the K value method) is applied to quantitatively analyze the content of minerals in the Xigeda formation claystones using MDI Jade 6 software. Based on the peak intensities and the peak intensity areas of all the minerals in the XRD pattern, the content of each mineral within the sample can be determined. The XRD test patterns show that the characteristic peaks of all mineral phases do not overlap, and the range of calculation error is ±5%. The XRD tests were conducted using a D/max-2500/PC X-ray diffractometer, produced by Rigaku company in Tokyo, Japan, equipped with a Ni filter and Cu-Kα radiation source at the Henan Rock and Mineral Testing Center, Henan Province, China. The scanning range was a 2θ angle of 3~60°, with a continuous scanning mode and a step size of 0.02°. The test conditions were set to 40 kV and 100 mA, while the ambient temperature was maintained at 24 °C with humidity levels at 36%.

3.3. Scanning Electron Microscope Tests

The scanning electron microscope (SEM) is a crucial instrument utilized for high-resolution micro-image analysis and is widely used in the study of the microstructure characteristics of rock and soil materials [28–30]. To examine the mineral morphology and pore structure of claystone samples, SEM was conducted using independently developed equipment by Beijing Zhongke Instrument Co., Ltd., Beijing, China. The equipment model is KYKY-EM6900LV, with a resolution of 3 nm at 30 kV (SE, high, low vacuum), continuous adjustable acceleration voltage ranging from 0 to 30 kV, and amplification ranging from 8 to 300,000 times. The yellow and gray claystone samples were sectioned, fractured, peeled, and sprayed with gold to prepare scanning electron microscope specimens. Representative scanning locations were chosen for imaging in a high-vacuum environment. The microstructure of claystone samples was quantitatively analyzed using Image-Pro Plus 6.0 (IPP) image analysis software. To avoid distortion at higher magnifications, SEM images with a magnification of 1500 times were selected for analysis in this study.

3.4. In-Situ Permeability Tests

The in-situ double-ring infiltration test is suitable for the silty and viscous soil layer above the water table [31,32]. The outer ring permeability field constrains lateral seepage,

ensuring high accuracy by allowing only vertical penetration of water in the inner ring. The test equipment offers the advantages of easy handling and installation, convenient and quick water injection, and accurate reading during testing [33]. To overcome operational challenges in complex mountainous regions, improvements were made to the test device by replacing the flow bottle and bottle holder with a measuring cup and cylinder, while readings are now conducted using a steel ruler (Figure 5). To investigate the permeability characteristics of Xigeda formation claystone in the study region, three representative test sites were selected (Figure 2). The in-situ double-ring infiltration tests were conducted in accordance with the water conservancy and hydropower engineering injection test procedures [34]. The main testing procedure involves (a) excavating a square test pit at the designated location and leveling the site. (b) The large and small rings are placed and sealed at their bases. A steel ruler is affixed to the outer wall of the small ring to ensure its verticality and proximity to the ground. (c) Water is simultaneously injected into both rings until a depth of 10 cm is reached. The stopwatch should be opened to start timing according to the specified requirements. Use the measuring cylinder to inject water into the two rings and maintain a liquid level of 10 cm. Record the volume of water added within a certain time period. Initially, measurements are taken every 5 min continuously for 5 times. Subsequently, measurements are taken every 15 min continuously for twice. Finally, measurements are taken every 30 min, with an additional small-scale test conducted six times.

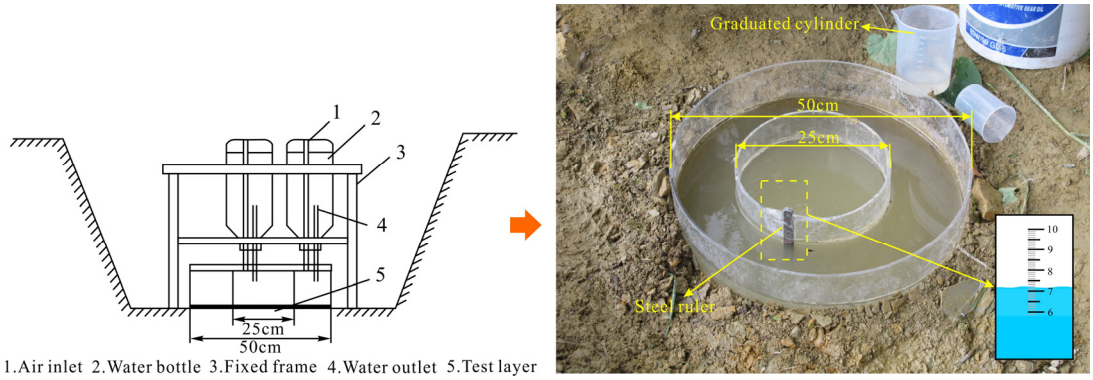

(a) In-situ double-ring infiltration test device (b) Picture of improved in-situ double-ring infiltration test

Figure 5. Double-ring infiltration test device and field test improvement (modified from Chen et al. [33]).

3.5. Triaxial Tests

Field investigation reveals that the yellow and gray claystones in the Xigeda formation of Haiziping Village, Luding County, exhibit low degrees of diagenesis, while their soil mass was significantly disturbed during sampling. To address this issue, remolded samples are utilized to conduct triaxial consolidation and undrained shear tests on both types of claystones under varying moisture content conditions. The yellow claystone samples were tested with moisture contents of 20%, 25%, and saturation, with the saturated moisture content measuring 30.93%. Similarly, the gray claystone samples were tested with moisture contents of 15%, 20%, and saturation, with the saturated moisture content measuring at 31.91%. The triaxial tests were conducted under each moisture condition while applying confining pressures of 100 kPa, 200 kPa, and 300 kPa. The triaxial tests were conducted using the TSZ automatic triaxial instrument at the Key Laboratory of Active Structure and Geological Safety, Ministry of Natural Resources.

4. Test Results

4.1. Mineral Composition

Figures 6 and 7 show the mineral composition of the yellow and gray claystone samples, respectively. The findings suggest that both samples share a similar mineral make-

up, primarily consisting of quartz and clay minerals with trace amounts of plagioclase, calcite, potash feldspar, siderite, and hornblende. However, there are noticeable differences in the proportion of each mineral.

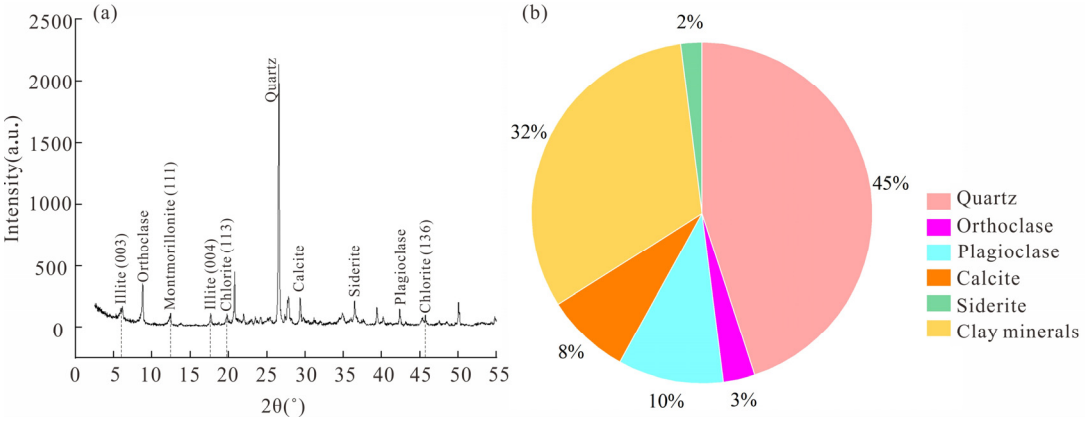

Figure 6. XRD analysis results of yellow claystone sample: (**a**) Characteristic peaks of identified minerals in XRD pattern; (**b**) Identified minerals composition and content.

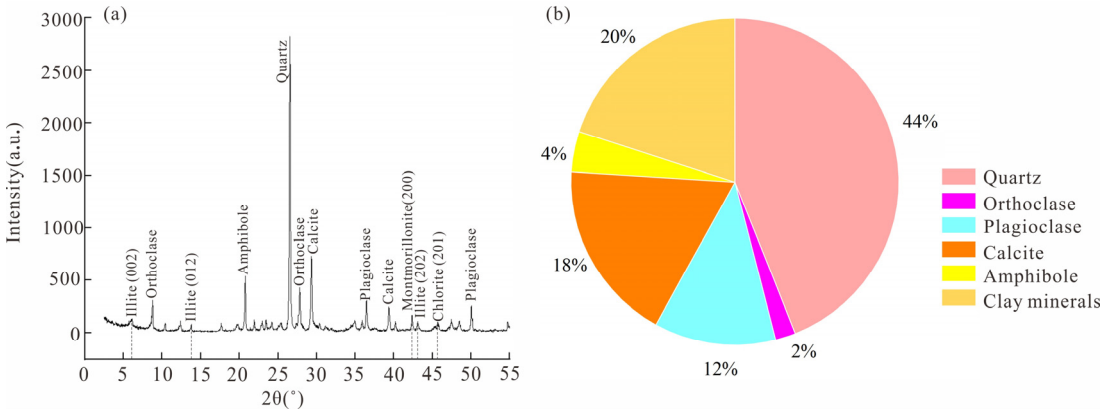

Figure 7. XRD analysis results of gray claystone sample: (**a**) Characteristic peaks of identified minerals in XRD pattern; (**b**) Identified minerals composition and content.

The yellow claystone exhibits a 12% higher content of clay minerals and a 10% lower content of calcite compared to the gray claystone, indicating more intense weathering and warm-wet climatic conditions during its deposition. In addition, the clay minerals in yellow and gray claystone samples are dominated by illite, accounting for 29.8% (±3%) and 17.8% (±3%), respectively, while the content of montmorillonite and chlorite is less (Table 2).

Table 2. XRD test results for minerals in yellow and gray claystone samples (wt.%).

Sample	Quartz	Orthoclase	Plagioclase	Calcite	Siderite	Hornblende	Clay Minerals				
							Montmorillonite	Montmorillonite—Illite Mixed Layer	Illite	Kaolinite	Chlorite
yellow claystone	45 (±4)	3 (±2)	10 (±4)	8 (±2)	2 (±1)	/	0.9 (±2)	/	29.8 (±3)	/	1.3 (±2)
gray claystone	44 (±3)	2 (±2)	12 (±3)	18 (±5)	/	4 (±1)	1.0 (±2)	/	17.8 (±3)	/	1.2 (±2)

Values represent wt.% of the mineral matter, with errors in parentheses.

4.2. Microstructure Characteristics

According to SEM images of claystones in their natural state, the yellow claystone exhibits a dense microstructure and is primarily composed of clastic rock particles and

fillings. Quartz predominates among the clastic particles, which range in size from 10 to 25 μm. Authigenic clay mineral aggregates are distributed along the edges of these clastic rock particles. The fillings consist mainly of illite and calcareous cement, with a minor amount of chlorite. Illite is intercalated in clastic rock particles' pores as sheets with a particle size ranging from 3 to 6 μm, while chlorite is foliated and attached to the edge of clastic rock particles. The cement is adhered to clay minerals, which are predominantly characterized by velvety and acicular structures that fill the pores (Figure 8). The gray claystone exhibits a loose microstructure with well-developed pores and small cracks, primarily composed of silty sand debris dominated by quartz particles ranging from 5 to 15 μm in size and flaky clay minerals, mainly illite, with particle sizes of 5 to 8 μm. The cementation of the clay minerals is weakly present and mainly fills the inter-granular sheet-like pores (Figure 9).

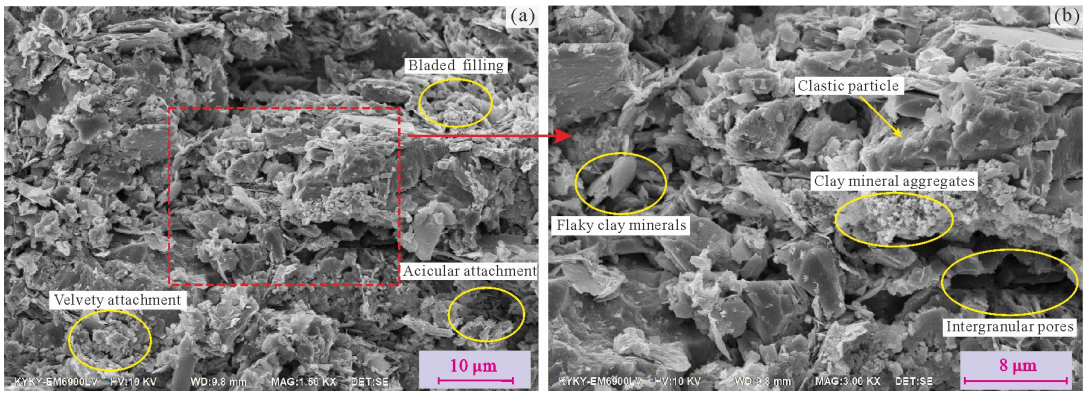

Figure 8. SEM image of yellow claystone sample: (**a**) The magnification is 1500 times; (**b**) The magnification is 3000 times.

The development of microstructural pores in the Xigeda formation effectively reflects the extent of external environmental interference during its deposition. By binarizing SEM images of soil samples, the identification of soil sample pores can be accurately achieved. These pores are then classified based on their size, facilitating quantitative statistics and analysis. Figures 10 and 11, respectively, show the SEM images of yellow and gray samples magnified 1500 times. By measuring the equivalent diameter (d), the pores in the claystone samples can be classified into four types: (1) large pores ($d > 4$ μm), (2) medium pores ($1 < d < 4$ μm), (3) small pores ($0.4 < d < 1$ μm), and (4) micro-pores ($d < 0.4$ μm). The results indicate that the micropores in the yellow and gray claystone samples are randomly distributed and independent, with a low connectivity rate. The gray claystone has more developed micropores compared to other samples (Figures 10b and 11b). The microporosity of yellow and gray claystone is predominantly micro- and small-sized, with medium-sized pores following closely behind. Large pores are not well-developed (Table 3), indicating that the hydrostatic sedimentary environment of the Xigeda formation in Haiziping Village, Luding County, was favorable and less susceptible to environmental disturbances during later periods.

The pore abundance (C) is defined as the ratio of the short axis length to the long axis length of the microstructured pore. The value of pore abundance (C) ranges from 0 to 1, with a higher value indicating a more circular or square-shaped porosity. The statistical results show that the distribution ranges of microstructure pore abundance value (C) in yellow and gray claystones exhibit high similarity, with the abundance value (C) being distributed across all intervals of the pore size. However, it is primarily concentrated within the 0.2~0.5 and 0.8~0.9 ranges (Figure 12). Notably, oblate pores are predominant in both yellow and gray claystones from the Xigeda formation in Haiziping Village, followed by equiaxed and strip types.

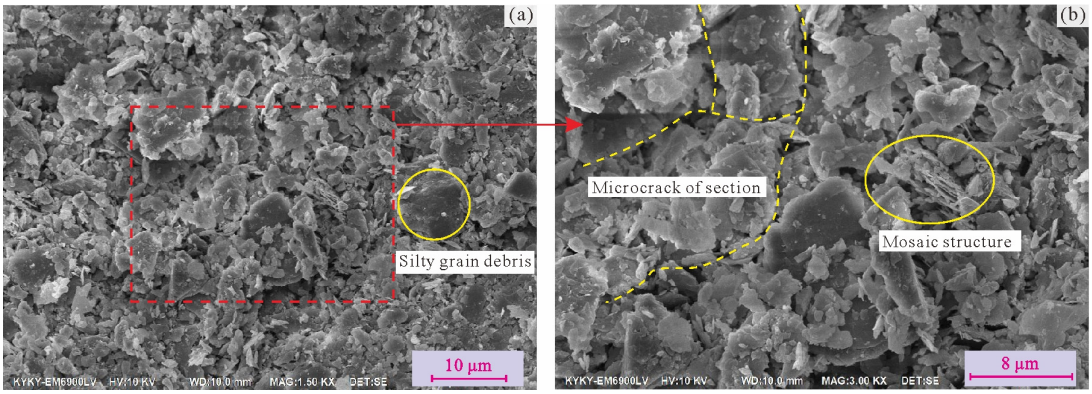

Figure 9. SEM image of gray claystone sample: (**a**) The magnification is 1500 times; (**b**) The magnification is 3000 times.

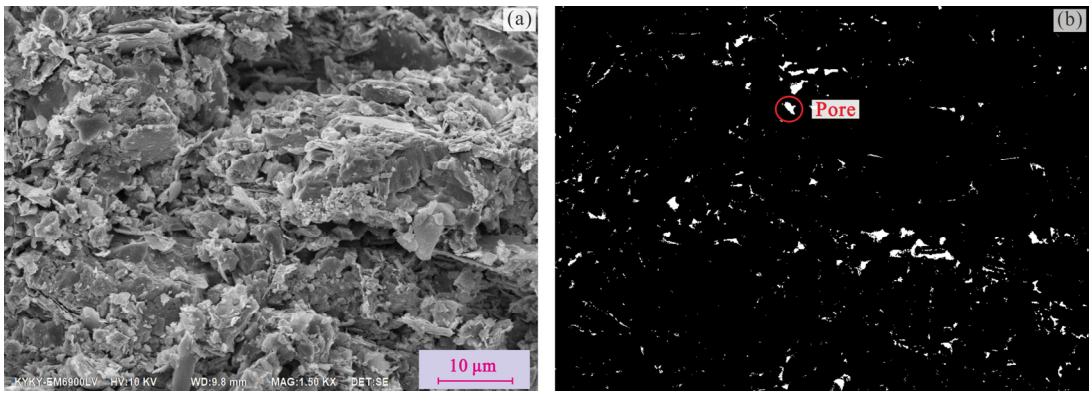

Figure 10. SEM image and binary image of yellow claystone sample: (**a**) The magnification is 1500 times; (**b**) Binary image.

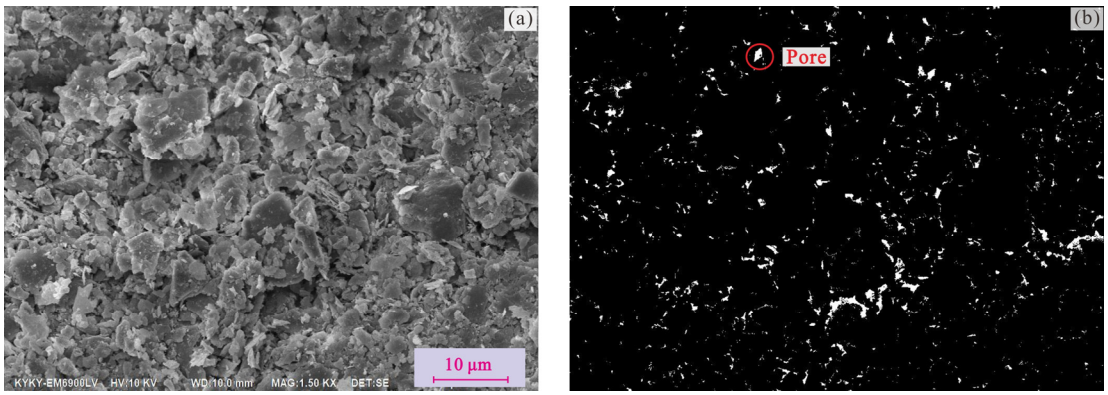

Figure 11. SEM image and binary image of gray claystone sample: (**a**) The magnification is 1500 times; (**b**) Binary image.

Table 3. Pore proportion of the Xigeda formation claystone samples.

Sample	Pore Proportion			
	<0.4 μm	0.4~1 μm	1~4 μm	>4 μm
Yellow claystone	69.13%	26.60%	4.27%	0
Gray claystone	71.01%	24.69%	4.16%	0.14%

The length of the blue rectangle represents the pore proportion of the claystone in different pore size intervals.

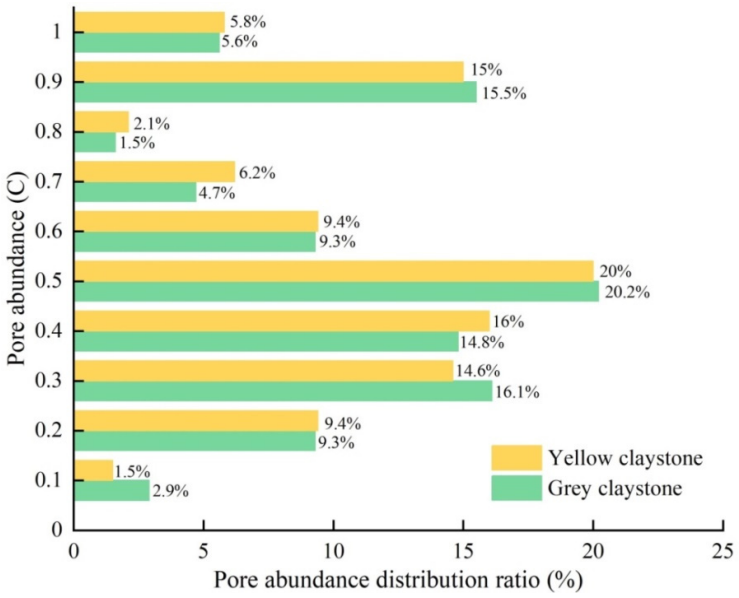

Figure 12. Distribution ratio of microscopic porosity of yellow and gray claystone samples.

4.3. Physical Properties

Table 4 presents the fundamental physical parameters of the yellow and gray claystone specimens, indicating that their basic physical characteristics are relatively similar. Specifically, the plasticity index of yellow claystone ranges from 7.8 to 14.2, while that of gray claystone varies between 8.4 and 12.9; both types belong to silt—silty clay.

Table 4. Physical parameters of the yellow and gray claystone samples.

No.	Sample	Moisture (%)	Soil Specific Gravity	Natural Density g/cm^3	Porosity	Liquid Limit %	Plastic Limit %	Plasticity Index	Saturated Moisture%
XGD-01	yellow	4.5	2.70	1.80	0.550	36.3	24.9	11.4	31.91
XGD-02	gray	3.7	2.69	1.86	0.569	36.4	25.9	10.5	30.93

In accordance with the Code of Water Injection Test for Water Resources and Hydropower Engineering [34], the in-situ double-ring infiltration tests were conducted at multiple outcropping points of the Xigeda formation in Haiziping Village (Figure 2). The resulting permeability coefficient ranged from 3.62×10^{-4} to 7.34×10^{-4} cm/s, with an average value of 5.11×10^{-4} cm/s, indicating a medium-permeable material (Table 5). Compared to the permeability characteristics of claystone in the Xigeda formation found in other regions, the test results obtained from Haiziping Village, Luding County, exhibit relatively higher values. This can be attributed to the environmental factors present in this region. Field investigation revealed that the diagenetic degree of this set of formations is low, while their integrity remains intact. However, the permeability of soil blocks without

microcracks or cracks is not developed, leading to an overestimation of the in-situ measured permeability coefficient for the Xigeda formation in Haiziping Village, Luding County.

Table 5. Results of double-ring water injection tests.

Test Number	Permeability Coefficient (cm/s)	Average Permeability Coefficient (cm/s)	Permeability Grade
S01	3.62×10^{-4}		
S02	7.34×10^{-4}	5.11×10^{-4}	medium permeability
S03	4.36×10^{-4}		

4.4. Mechanical Properties

Figure 13 illustrates that the peak shear strength of the yellow and gray claystone samples decreases as moisture content increases under identical confining pressure conditions. Within the range of tested moisture content, there exists a positive linear correlation between peak strength and moisture content. The cohesion of the two claystone samples exhibited a decreasing trend with increasing moisture content, and this decrease was more pronounced at higher moisture contents, as shown in Figure 14. When the moisture content of the yellow claystone increased from 20% to its saturated state (30.93%), the cohesion decreased by 84.7%, dropping from 121.12 kPa to 18.54 kPa. Similarly, when the moisture content of gray claystone increased from 15% to its saturated state (31.91%), the cohesion decreased by 99.2%, plummeting from 50.98 kPa to a mere 0.4 kPa. In addition, the yellow claystone exhibits a significantly higher degree of cohesion compared to its gray counterpart. This observation further supports the notion that cementation between clay minerals in yellow claystone is stronger and more compactly structured. However, as moisture content increases, this cementation structure becomes increasingly susceptible to damage, leading to a significant reduction in cohesion.

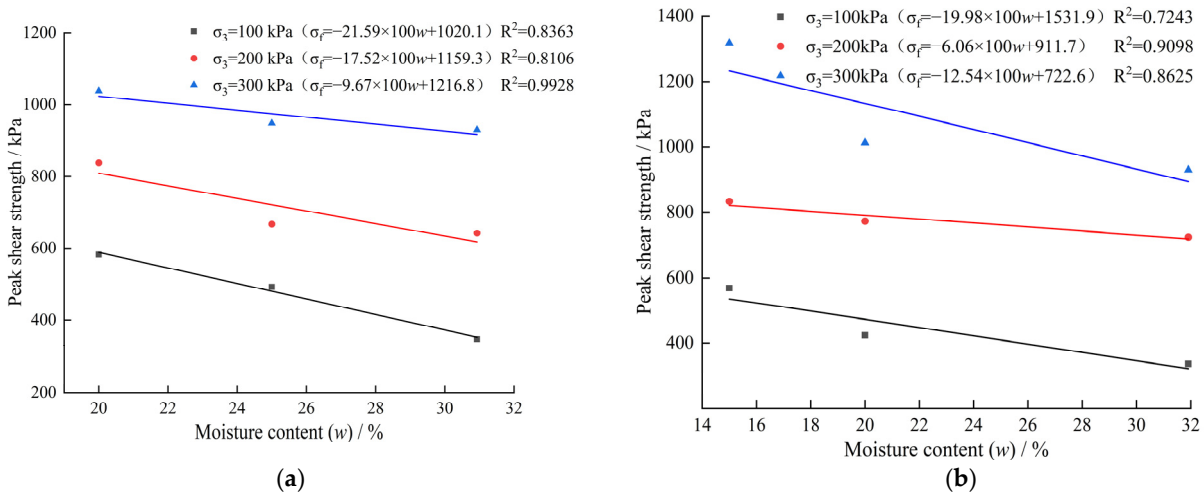

(**a**) (**b**)

Figure 13. Relationship between peak shear strength and moisture content of claystone samples under different confining pressures: (**a**) Yellow claystone sample; (**b**) Gray claystone sample.

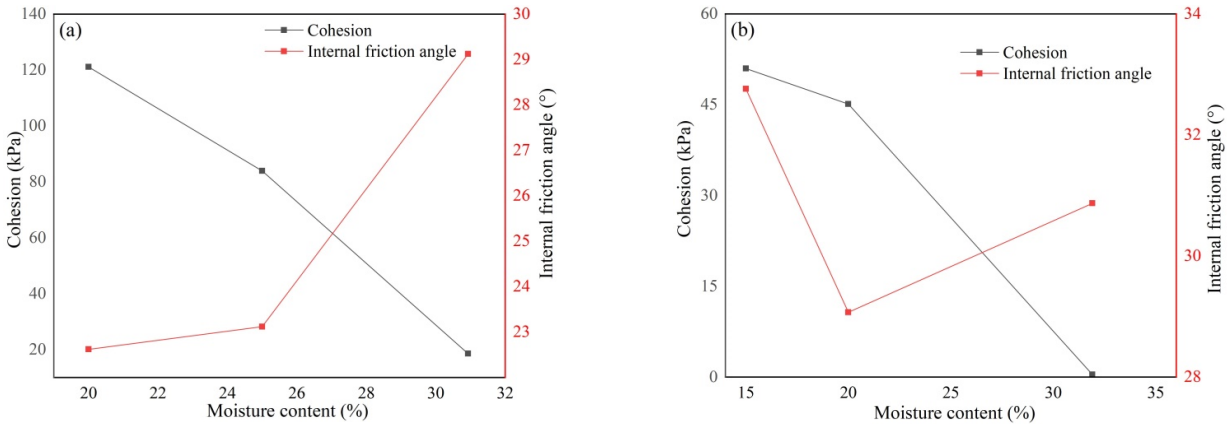

Figure 14. Relationship between cohesive strength, internal friction angle, and moisture content of claystone samples: (**a**) Yellow claystone sample; (**b**) Gray claystone sample.

When the moisture content increases, the internal friction angle of yellow claystone gradually increases. Specifically, as the moisture content rises from 20% to saturation (30.93%), there is a corresponding increase in internal friction angle from 22.62° to 29.12°, representing a significant rise of 28.7%. However, the internal friction angle of gray claystone exhibited a non-monotonic variation trend with respect to moisture content. The magnitude of change was relatively small, and the difference in internal friction angle between soil samples with different moisture contents fluctuated within ±4°. When the claystone sample had a low moisture content, water filled the micropores and formed a lubricating film between particles. As the moisture content increases, the cohesive force gradually weakens while the interaction between rock clastic particles strengthens, leading to a gradual increase in the internal friction angle.

5. Discussions

5.1. Hydrologic Characteristics of the Xigeda Formation in Different Regions

Based on the existing research and the test results presented in this study [35], it is evident that the limit moisture content of claystone within the Xigeda formation at Haiziping Village, Luding County, is generally lower than that observed in the Panxi region. Additionally, it was found that its plasticity index is significantly lower than that of the latter (Figure 15). Since the liquid limit moisture content of soil is positively correlated with its clay mineral content, it can be inferred that the clay mineral content of the claystones in the Xigeda formation in Haiziping Village, Luding County, is lower than that in the Panxi area.

Comparative analysis of the permeability characteristics of the Xigeda formation in different regions reveals that the permeability coefficient order of magnitude for claystone in Haiziping Village is comparable to that of siltstones in other regions, both being 10^{-4} cm/s, which is significantly higher than that of claystone found elsewhere (which mainly ranges from 10^{-5}~10^{-7} cm/s) (Table 6). It can be seen from this that the permeability characteristics of the claystones in the Xigeda formation in Haiziping Village are roughly equivalent to those of the siltstones in the Xigeda formation in other regions but greater than those of the clays/rocks. It can be inferred that the permeability properties of claystones in the Xigeda formation in Haiziping Village are roughly comparable to those of siltstones found in other regions within the same formation, yet superior to those of pure clay. The permeability characteristics of the Xigeda formation exhibit significant variations across different regions and lithologies, which may be closely associated with factors such as testing methodologies, regional geological conditions, diagenetic processes, and post-depositional disturbances.

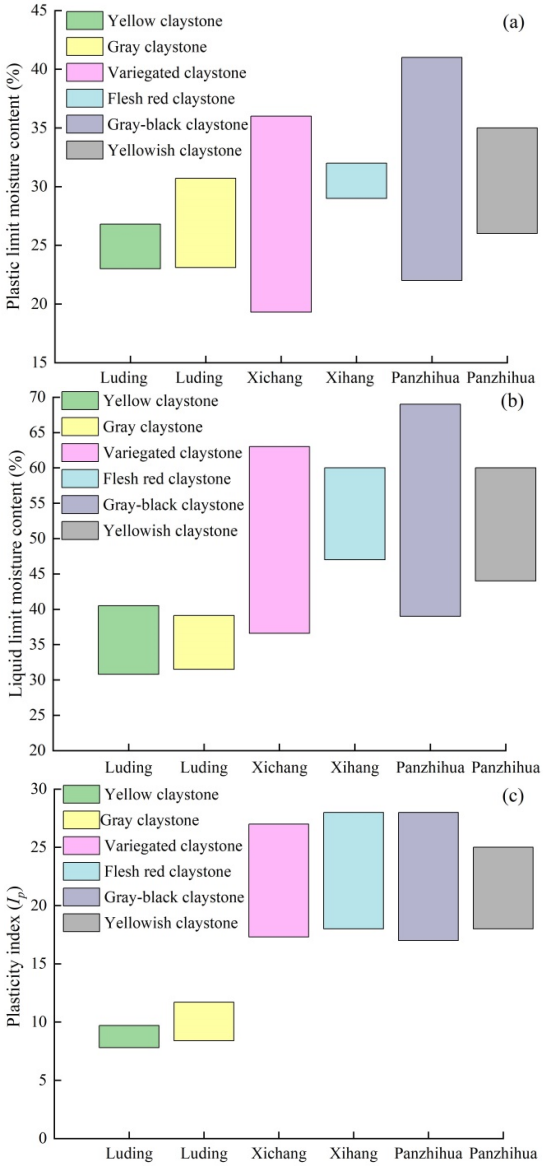

Figure 15. Limit moisture content of Xigeda formation in different regions of China: (**a**) Plastic limit moisture content; (**b**) Liquid moisture limit; (**c**) Plasticity index.

5.2. Strength Characteristics of the Xigeda Formation in Different Regions

The comparative analysis of the mechanical strength indices of the Xigeda formation in different regions of southwestern China [11,17–20,41], reveals that the cohesiveness of silt-subclay in Haiziping Village, Luding County, is comparatively lower than that of semi-diagenetic clay/rock in Zhaizi Village, Yunnan Province, and Panxi area, Sichuan Province. However, it is higher than that of siltstones in the Panxi area. The internal friction angle in Xinjiu Township of Panzhihua City is slightly lower than that of sandstones but higher than that of semi-diagenetic clays and siltstones in other regions (Figure 16).

The cohesion of the Xigeda formation in different regions decreases with an increase in moisture content, with varying degrees of sensitivity observed. With the increase in moisture content, the water sensitivity of claystone cohesion is most significant in Haiziping Village, Luding County, followed by semi-diagenetic rocks in Zhaizi Village, Yunnan Province. The water sensitivity of sandstones in the Panxi area is comparatively weaker (Figure 16a). In addition, the internal friction angle of Xigeda formations in other regions decreases with increasing moisture content, whereas that of claystone in the Luding area increases with increasing moisture content. With the increase in moisture content, the internal

friction angle of the claystone at Haiziping Village, Luding County, increases significantly more than that of semi-diagenetic clay/rock in Zhaizi Village, Yunnan Province, and Panxi area, where it decreases most prominently. The internal friction angle of clay/rock in the Panxi area experiences the smallest decrease (Figure 16b). From the aforementioned analysis, it is evident that there exist regional and lithological disparities in the susceptibility of Xigeda formations to variations in moisture content across different regions. Among these, the claystone in the Haiziping area of Luding County exhibits the most pronounced sensitivity with respect to mechanical properties influenced by moisture content, while the clay in the Panxi area displays the greatest degree of sensitivity. Additionally, the clay/rock located in the Panxi area of Sichuan Province and the semi-diagenetic rocks located in Zhaizi Village, Yunnan Province, exhibit a higher level of sensitivity than the sandstones found within the Panxi area.

Table 6. Comparison of permeability characteristics of Xigeda formation in different regions.

Site	Test Subject	Test Conditions	Permeability Coefficient (cm/s)	Permeability Classification	Data Sources
Luding Haiziping	claystone	on-site double-ring water injection	$3.62\sim7.34 \times 10^{-4}$	medium	this paper
Panzhihua Griping	silty clay	indoor penetration	$3.7 \times 10^{-5}\sim7.2 \times 10^{-4}$	impermeable	Reference [36]
	siltstone	indoor penetration	$2.0\sim2.78 \times 10^{-5}$	impermeable	Reference [37]
Panzhihua Suziping	silty clay	indoor penetration	$2.8\sim3.3 \times 10^{-7}$	very weak	Reference [38]
Longkou Town, Yunnan Province	claystone	indoor penetration	$10^{-8}\sim10^{-7}$	very weak	Reference [39]
Southern Sichuan	mudstone	field, indoor penetration	$1.7\sim5.25 \times 10^{-5}$	impermeable	Reference [40]
	sandstone		1.6×10^{-4}	medium	
Xichang Jingjiu Township	claystone	indoor penetration, borehole pressurized water	$1.95 \times 10^{-7}\sim4.61 \times 10^{-5}$	impermeable	Reference [41]
	siltstone		$1.47\sim6.54 \times 10^{-4}$	medium	

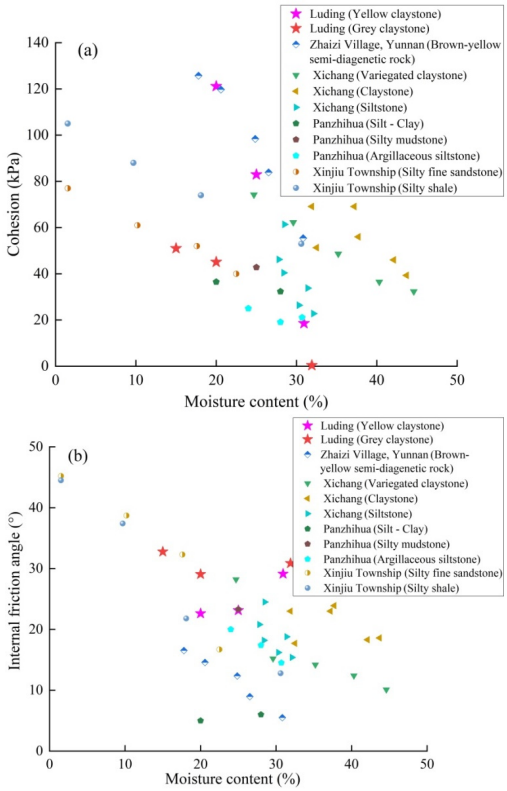

Figure 16. Relationship between strength index and moisture content of Xigeda formation in different regions: (**a**) Cohesion; (**b**) Internal friction angle.

6. Conclusions

Accurate characterization of the engineering geological properties of the Xigeda formation is imperative for conducting a comprehensive stability analysis, given its typical composition of hard soil or soft rock. In this study, we conducted field investigations and various tests, including XRD, SEM, permeability tests, physical property tests, and mechanical tests, on the Xigeda formation located in Haiziping Village along the Dadu River. By analyzing their microstructure and mechanical properties and comparing them with the engineering geological characteristics of other Xigeda formation in southwestern China, the following conclusions are drawn:

(1) The Xigeda formation claystones in Haiziping Village, Luding County, are composed of fine-grained materials such as silt and clay, resulting from the interbedding of yellow and gray claystones. The material composition of yellow and gray claystones primarily comprises quartz and clay minerals, with illite being the predominant type of clay mineral. The microstructure of the yellow and gray claystones displays significant disparities. The cement structure of the clay minerals in the yellow claystone is conspicuous, whereas the clay minerals in the gray claystone appear thin and scattered. In terms of microstructure, the yellow claystone exhibits higher density and stronger cementation between its clay minerals compared to the gray claystone;

(2) The cohesion of yellow and gray claystones exhibits a negative correlation with moisture content, while the internal friction angle displays a positive correlation with moisture content. The micro-mechanism can be explained as the disruption of cementation structure in clay minerals due to their interaction with water, leading to a gradual loss of cohesion. Meanwhile, the interaction between rock clastic particles results in an increase in internal friction angle, which is more significant under high moisture content conditions;

(3) There are significant differences in the hydraulic and mechanical properties of the Xigeda formation in different regions. The permeability of yellow and gray claystones in Luding County falls within the range observed for sandstone and claystone within the Panxi regions of Sichuan Province. Moreover, the cohesion of the Xigeda formation claystones in Haiziping Village, Luding County, is intermediate between that of sandstone, semi-diagenetic rock, and claystone found elsewhere. Moreover, its internal friction angle exceeds that of semi-diagenetic rock and clay but resembles that of sandstone;

(4) The mechanical properties of the Xigeda formation exhibit a gradual decline in different regions as moisture content increases, with variations in water sensitivity observed across lithologies and locales. Notably, the claystone within the Xigeda formation located in Luding County displays the most significant susceptibility to water.

Author Contributions: Conceptualization, R.W. and C.G.; methodology, R.W. and X.L.; software, X.L.; writing—original draft preparation, R.W., X.L. and C.Q.; experiment, J.N., Y.W., D.S. and X.L.; supervision, R.W. and C.G. All authors have read and agreed to the published version of the manuscript.

Funding: This research was funded by [National Key Research and Development Program of China] grant number [2021YFC3000505], [National Natural Science Foundation of China] grant number [42207233 and 42007280], and [China Geological Survey projects] grant number [DD20221816].

Institutional Review Board Statement: Not applicable.

Informed Consent Statement: Not applicable.

Data Availability Statement: Not applicable.

Acknowledgments: The authors would like to thank Zhihua Yang, Xue Li, and Ning Zhong from the Institute of Geomechanics, Chinese Academy of Geological Sciences, and doctoral candidate Caihong Li from the China University of Geosciences (Beijing) for their kind support during the

field investigation. We gratefully acknowledge the three anonymous reviewers and editor for their valuable revision suggestions, which greatly improved the quality of the article.

Conflicts of Interest: The authors declare no conflict of interest.

References

1. Rocha, M. Some problems related to rock mechanics of low resistance. *Inecmemoria* **1977**, *491*, 1.
2. Bienawsky, T. Felsklassifkation: Stand der Technick und Moglichkeiten der Normung. *Anon. Forschungsberichte Transportwesens* **1981**, 2–9.
3. Grainger, P. The classification of mudrocks for engineering purpose. *Q. J. Eng. Geol. Hydrogeol.* **1984**, *17*, 381–387. [CrossRef]
4. Johnston, I.W. Strength of Intact Geomechanical Materials. *J. Geotech. Eng.* **1985**, *111*, 730–749. [CrossRef]
5. Johnston, I.W.; Novello, E.A. Soil mechanics, rock mechanics and soft rock technology. *Geotech. Eng.* **1994**, *107*, 3–9. [CrossRef]
6. Kanji, M.A.; Leão, M. Correlation of Soft Rock Properties. In *Soft Rock Mechanics and Engineering*; Springer Nature Switzerland AG: Cham, Switzerland, 2020; pp. 407–421.
7. Duhović, A.; Cvitanović, N.S.; Vlastelica, G.; Török, A. Marly Soft Rocks: Correlation of Physical and Mechanical Properties-Examples from Dalmatia (Croatia) and Budapest (Hungary). *Symmetry* **2022**, *14*, 2173. [CrossRef]
8. Guzzetti, F.; Cardinali, M.; Reichenbach, P. The influence of structural setting and lithology on landslide type and pattern. *Environ. Eng. Geosci.* **1996**, *II*, 531–555. [CrossRef]
9. Vondráčková, T.; Musílek, J.; Kais, L. The Issue of Soft Rocks Causing Problems in Foundation Engineering. *Procedia Earth Planet. Sci.* **2015**, *15*, 54–59. [CrossRef]
10. Erharter, G.H.; Poscher, G.; Sommer, P.; Sedlacek, P. Geotechnical characteristics of soft rocks of the Inneralpine Molasse—Brenner Base Tunnel access route, Unterangerberg, Tyrol, Austria. *Geomech. Tunnelbau* **2019**, *12*, 716–720. [CrossRef]
11. Du, Y.X.; Sheng, Q.; Fu, X.D.; Dan, L.Z.; Zhang, Z.P.; Du, W.J.; Chen, H. Study on deformation and strength characteristics and damage constitutive model of semi-diagenetic rocks. *Chin. J. Rock Mech. Eng.* **2020**, *39*, 239–250.
12. Jiang, F.C.; Wu, X.H.; Xiao, H.G. The age of Xigeda Formation in Luding, Sichuan and its neotectonic significance. *Acta Geol. Sin.* **1999**, *1*, 190. (In Chinese)
13. Kong, P.; Darryl, E.G.; Wu, F.Y.; Caffee, M.W.; Wang, Y.J. Cosmogenic nuclide burial ages and provenance of the Xigeda paleo-lake: Implications for evolution of the Middle Yangtze River. *Earth Planet. Sci. Lett.* **2009**, *278*, 131–141. [CrossRef]
14. Deng, B.; David, C.; Mark, C.; Liu, S.; Nathan, C.; Lei, J.; O'Sullivan, G.; Li, Z.W.; Li, J.X. Late Cenozoic drainage reorganization of the paleo-Yangtze river constrained by multi-proxy provenance analysis of the Paleo-lake Xigeda. *Bull. Geol. Soc. Am.* **2020**, *133*, 199–211. [CrossRef]
15. Zhou, P.; Zhou, F.C.; Jiang, Y.F.; Li, J.Y.; Lin, J.Y.; Lin, M.; Wang, Z.J. Study on the mechanism of tunnel catastrophe in Xigeda formation considering the interbed effect. *Chin. Tunn. Undergr. Space Technol.* **2023**, *135*, 105054. [CrossRef]
16. Xu, Y.Z.; Fan, X.Y.; Zhang, Y.Y.; Tian, S.Y.; Wen, X.; Liu, H.N.; Zheng, Y.F.; Liao, H.K. Numerical analysis on dynamic characteristics of Zhonghai Village landslide in HanyuanCounty of Sichuan Province. *Geol. Surv. China* **2022**, *9*, 102–111. (In Chinese)
17. Zhang, W.; Xu, Z.M.; Liu, W.L.; Li, L. Study on the influence of water content to shear strength of Xigeda-strata clay rock in Xichang. *Geotech. Investig. Surv.* **2011**, *39*, 1–5. (In Chinese)
18. An, S.P.; Wei, L.D.; Liu, W.L.; Zhang, X.L. Experimental study on mechanical behavior of Xigeda Formation siltstone and structure interface. *J. Eng. Geol.* **2013**, *21*, 702–708. (In Chinese)
19. Lu, Z.P.; Kong, Y.X.; Wang, H.J.; Tang, H.W. Compressive characteristics and microstructure of Xigeda soil. *J. Nanjing Univ. Technol. (Nat. Sci. Ed.)* **2022**, *44*, 114–122. (In Chinese)
20. Song, D.G.; Wu, R.A.; Ma, D.Q.; Guo, C.B.; Wang, Y.; Ni, J.W.; Li, X. Simulation analysis of landslide disaster movement process in Xigeda Formation, Luding County, Sichuan Province. Geol. Bull. China. 2022. Available online: https://kns.cnki.net/kcms/detail/11.4648.P.20220512.1451.004.html (accessed on 19 July 2023). (In Chinese).
21. Chen, Z.L.; Sun, Z.M.; Royden, L.H.; Zhang, X.Y. Landslide blocked lake: Origin of the Xigeda Formation in Luding, Sichuan and its significance. *J. Quat. Sci.* **2004**, *24*, 614–620.
22. Wang, P.; Li, J.P.; Wang, J.C.; Liu, C.R.; Han, F.; Gao, L. Quartz Ti-center in ESR dating of Xigeda Formation in Sichuan and contrast with magnetic stratigraphic profiles. *Nucl. Technol.* **2011**, *34*, 111–115. (In Chinese)
23. Shi, Y.Y. Cosmogenic nuclides Isochronal burial dating and geomorphological significance of the Haiziping Xigeda Formation in Luding section of Dadu River. Ph.D. Thesis, Nanjing Normal University, Nanjing, China, 2020. (In Chinese).
24. Wang, Y.S.; Wu, J.F. The characteristics and mechanism of large scale landslides between Huangjinping and Detuo in Daduhe river. *Adv. Mater. Res.* **2011**, *243–249*, 3211–3216.
25. Wu, L.Z.; Deng, H.; Huang, R.Q.; Zhang, L.M.; Guo, X.G.; Zhou, Y. Evolution of lakes created by landslide dams and the role of dam erosion: A case study of the Jiajun landslide on the Dadu River, China. *Quat. Int.* **2019**, *503*, 41–50. [CrossRef]
26. *GB/T 50123-2019*; Standard for Geotechnical Test Methods. Ministry of Housing and Urban-Rural Development: Beijing, China, 2019. (In Chinese)
27. Ruffell, A.; Wiltshire, P. Conjunctive use of quantitative and qualitative X-ray diffraction analysis of soils and rocks for forensic analysis. *Forensic Sci. Int.* **2004**, *145*, 13–23. [CrossRef]

28. Farulla, C.A.; Rosone, M. Microstructure characteristics of unsaturated compacted scaly clay. In *Unsaturated Soils: Research and Applications*; Springer: Berlin/Heidelberg, Germany, 2012; Volume 1, pp. 123–130.
29. Yoobanpot, N.; Jamsawang, P.; Horpibulsuk, S. Strength behavior and microstructural characteristics of soft clay stabilized with cement kiln dust and fly ash residue. *Appl. Clay Sci.* **2017**, *141*, 146–156. [CrossRef]
30. Gonzalez-Blanco, L.; Romero, E.; Pinyol, N.M.; Alonso, E.E. Microstructure of compacted low-plasticity soils: The initial fabric and its evolution on stress and suction paths. *E3S Web Conf.* **2023**, *382*, 11003. [CrossRef]
31. Verbist, K.; Torfs, S.; Cornelis, W.M.; Oyarzun, R.; Soto, G.; Gabriels, D. Comparison of single- and double-ring Infiltrometer methods on stony soils. *Vadose Zone J.* **2010**, *9*, 462–475. [CrossRef]
32. Faridah, S.N.; Achmad, M.; Jamaluddin, T.A.; Jusmira. Infiltration model of mediterranean soil with clay texture. *J. Tek. Pertan. Lampung* **2023**, *12*, 162–173. [CrossRef]
33. Chen, Z.H.; Chen, S.J.; Chen, J.; Sheng, Q.; Min, H.; Hu, W. In-situ Double-Ring Infiltration Test of Soil-Rock Mixture. *J. Yangtze River Sci. Res. Institude* **2012**, *19*, 52–56. (In Chinese)
34. *SL345-2007*; Code of Water Injection Test for Water Resources and Hydropower Engineering. Ministry of Water Resources of the People's Republic of China: Beijing, China, 2007. (In Chinese)
35. Wang, S.J.; Huang, D.C. *Environmental Engineering Geology in West of Sichuan*; China Ocean Press: Beijing, China, 1990. (In Chinese)
36. Song, W.G.; Du, Y.P. On dam anti-seepage material test with Xigeda soil. *Shanxi Archit.* **2017**, *43*, 228–229. (In Chinese)
37. Zuo, Y.Z.; Zhang, W.; Zhang, X.C.; Dang, C. Engineering properties of Xigeda strata siltstone as the filling material of earth-rock dam. *J. Yangtze River Sci. Res. Inst.* **2016**, *33*, 84–88. (In Chinese)
38. Li, X.Q. Engineering characteristics of Xigeda foundation soil in Suziping Hydropower plant. *Guangxi Water Resour. Hydropower Eng.* **1996**, *1*, 18–22+45. (In Chinese)
39. Zhang, D.Q.; Sun, X.W.; Wei, S.C.; Wang, J.Y. Study on physical properties of Xigeda clay at Longkaikou Hydropower Station in the middle reaches of Jinsha River. *Yangtze River* **2021**, *52*, 104–107. (In Chinese)
40. Zhong, C.; Fan, D.P. Study on engineering geological characteristics of Xigeda Formation in south Sichuan. *Sichuan Water Power* **2012**, *31*, 97–99. (In Chinese)
41. Yang, B.; Fan, Z.G.; Liu, W.L.; Xu, L.D. Engineering property of Xigeda strata of Panzhihua new steel V-Ti base. *Sci. Technol. Eng.* **2010**, *10*, 973–976. (In Chinese)